scientific reports

OPEN

Rational Sine-Gordon expansion method to analyze the dynamical behavior of the time-fractional phi-four and (2 + 1) dimensional CBS equations

Abdulla-Al- Mamun[1,2,3], Chunhui Lu[1,2], Samsun Nahar Ananna[4] & Md Mohi Uddin[5]

This study uses the rational Sine-Gordon expansion (RSGE) method to investigate the dynamical behavior of traveling wave solutions of the water wave phenomena for the time-fractional phi-four equation and the (2 + 1) dimensional Calogero-Bogoyavlanskil schilf (CBS) equation based on the conformable derivative. The technique uses the sine-Gordon equation as an auxiliary equation to generalize the well-known sine-Gordon expansion. It adopts a more broad strategy, a rational function rather than a polynomial one, of the solutions of the auxiliary equation, in contrast to the traditional sine-Gordon expansion technique. Several explanations for hyperbolic functions may be produced using the previously stated approach. The approach mentioned above is employed to provide diverse solutions of the time-fractional phi-four equation and the (2 + 1) dimensional CBS equations involving hyperbolic functions, such as soliton, single soliton, multiple-soliton, kink, cusp, lump-kink, kink double-soliton, and others. The RSGE approach enhances our comprehension of nonlinear processes, offers precise solutions to nonlinear equations, facilitates the investigation of solitons, propels the development of mathematical tools, and is applicable in many scientific and technical fields. The solutions are graphically shown in three-dimensional (3D) surface and contour plots using MATLAB software. All screens display the absolute wave configurations in the resolutions of the equation with the proper parameters. Furthermore, it can be deduced that the physical properties of the found solutions and their characteristics may help us comprehend how shallow water waves move in nonlinear dynamics.

Keywords The rational sine-Gordon expansion (RSGE) method, Phi-four equation, Soliton wave, Travelling wave solution, Calogero-Bogoyavlanskil Schilf equation, Sine-Gordon, Water wave

To characterize the physical properties of various applied science problems, such as fluid dynamics, hydrodynamics, plasma physics, and quantum mechanics, given the right circumstances, ordinary and partial differential equations may be used to represent the problems. Analytical solutions to partial differential equations (PDEs), particularly nonlinear equations, are more complex than those to ordinary differential equations (ODEs). PDEs frequently transform into ODEs using the Ansatz (direct) and Symmetry approaches to look for explicit solutions. Exact solutions help compare numerical systems and confirm accuracy. The endeavor to get precise, analytical solutions to PDEs is not just of an academic nature; it holds practical importance in verifying and comparing numerical and simulation techniques. In applied sciences, precise mathematical models and solutions are essential when doing direct experiments, which may be difficult or unfeasible. Although exact solutions are beneficial, they are infamously challenging for most nonlinear partial differential equations (PDEs), which are commonly

[1]College of Hydrology and Water Resources, Hohai University, Nanjing 210098, People's Republic of China. [2]State Key Laboratory of Hydrology-Water Resources and Hydraulic Engineering, Hohai University, Nanjing, People's Republic of China. [3]Department of Computer Science and Engineering, Northern University of Business and Technology Khulna, Khulna 9100, Bangladesh. [4]School of Mathematics, Hohai University, Nanjing 210098, People's Republic of China. [5]College of Water Conservancy and Hydropower Engineering, Hohai University, Nanjing 210098, People's Republic of China. email: abdullamamun21@nubtkhulna.ac.bd; abdullamamun21@gmail.com

used to represent real-world processes. The complexity derives from the inherent nonlinearity, which frequently gives rise to intricate phenomena like chaos, turbulence, and wave breaking, which lack straightforward analytical explanations. Despite the difficulties, current research in mathematical methods, computational techniques, and theoretical physics is still progressing and increasing the number of partial differential equations (PDEs) for which we have exact solutions or effective approximation methods. This improves our understanding and ability to model complex systems in applied sciences.

The $(2+1)$-dimensional CBS equation is a nonlinear partial differential equation and can exhibit various solutions, including solitons, rogue waves, and other nonlinear wave patterns. It has applications in studying multiple physical systems, including fluid dynamics, plasma physics, and nonlinear optics. Consider the subsequent generalized $(2+1)$-dimensional CBS circumstances:

$$u_t + \phi(u)u_y = 0, \phi(u) = \partial_x^2 + au + bu_x\partial_x^{-1}, \tag{1}$$

or homogeneously,

$$u_t + u_{xxy} + auu_y + bv_x\partial_x^{-1}v_y = 0, \tag{2}$$

where $\partial_x^{-1} = \int f dx$ and a, b are constraints. Equation (2) can be characterized in the probable time-fractional form of the CBS equation[1,2].

$$u_x D_t^{\theta} u + 4u_x u_{xy} + 2u_{xx}u_y + u_{xxxy} = 0, t > 0, x, y \in \mathbb{R}, \tag{3}$$

where $0 < \theta \leq 1$.

The time-fractional Phi-Four equation is a partial differential equation that generalizes the standard Phi-Four equation by incorporating fractional derivatives concerning time. The standard Phi-Four equation is a well-known equation in mathematical physics, often used to describe certain phenomena in fields like condensed matter physics and nonlinear optics. Adding fractional derivatives in time allows for more complex behaviors that capture specific anomalous diffusion processes. Due to the inclusion of fractional derivatives, the behavior, and solutions of the time-fractional Phi-Four equation can be more intriguing and complex than those of the ordinary Phi-Four equation. Anomaly diffusion and other unusual behaviors may result from the non-locality and memory effect introduced by the fractional derivative. The Phi-four equation is a specific form of the Klein–Gordon equation[1].

$$D_t^{2\theta} u - u_{xx} + \lambda^2 u + \mu u^3 = 0, \gamma > 0, 0 < \theta \leq 1 \tag{4}$$

where λ and μ are real numbers.

The main goal of this work is to directly apply the RSGE method to the dynamical analysis of the time-fractional phi-four equation and the $(2+1)$ dimensional CBS equation. There are several benefits when comparing our strategy to the other approaches. Simply put, it employs a more structured technique and more steps to generate an algebraic system. It also automatically creates kink and singular soliton solutions[3–5]. The principal important methodology of this method is too explicit the exact solutions of FNLEEs that satisfy the Nonlinear ODE of the form, $U(\psi) = \sum_{i=1}^{N} \tanh^{i-1}\psi(a_i\mathrm{sech}\psi + c_i\tanh\psi + a_0)/\sum_{i=1}^{N} \tanh^{i-1}\psi(b_i\mathrm{sech}\psi + d_i\tanh\psi + b_0)$. Our method provides a more direct and concise approach to the exact travelling wave solution than the other existing systems. Some authors used this RSGE technique to determine the exact solution to multiple NLEEs in the deferential sense of derivative, such as Jumarie's modified Riemann–Liouville derivatives, conformable derivatives, and Kerr law nonlinearity. Nevertheless, no adequate studies utilizing this method have been conducted on our suggested time-fractional phi-four equation and the $(2+1)$ dimensional CBS equation. Here, the recently found exact solution of the time-fractional phi-four equation and the $(2+1)$ dimensional CBS equations is more accurate, efficient, and versatile enough to be used in many treatments in mathematical physics, engineering, and wave analysis. Thus, we can state that our proposed research is innovative in the sense of conformable derivatives as it employs the RSGE technique to dynamically analyze the time-fractional phi-four equation and the $(2+1)$ dimensional CBS equation. We presented the results using the mathematical software Mathematica by choosing appropriate values for the employed parameters and then employing illustrations to simplify the physical interpretation suitably.

To establish a flow in a domain, air must be replaced by water in soils (and foams), or vice versa, in fluid recovery activities. The principles governing fluid flow are the same in both systems. However, depending on the media, these regulations may be conveyed differently or utilize different languages. Although the scientific fields of flow in soil and flow in foam are concerned with similar physical laws[6–8], communication between them has been impeded by a lack of common vocabulary. Water waves are a regular and fascinating example of traveling waves in nature. As a traveling wave passes over the water's surface, the water's surface oscillates up and down, creating wave patterns that move over the top. How water waves behave may be determined by their properties, including their wavelength, frequency, speed, and amplitude. The wave equation governs the dynamics of water waves, a partial differential equation that explains the relationship between wave motion, time, and space. The standard wave equation for small-amplitude waves in shallow water is the one-dimensional linear shallow water wave equation, sometimes referred to as the Korteweg-de Vries equation (KdV)[9]. It describes waves with a single wave profile and the ability to move without changing shape. In water, waves frequently disperse, which means they move at varied speeds depending on their wavelength. Longer waves with lower frequencies travel more quickly than shorter waves with higher frequencies.

This dispersion results from the waves' interactions with the surface tension, water depth, and waves. For waves with large amplitudes propagating over great distances, the dynamics of water waves can become nonlinear[10]. Rogue waves and solitons are intricate patterns that can develop due to nonlinear wave dynamics. Waves may get steeper and more unstable as they approach shallow water, eventually breaking into choppy whitecaps. This phenomenon is most noticeable near coastlines. Water waves, in general, show a wide variety of features, making them a significant subject of interest and research in fluid dynamics, oceanography, and other related fields. Wave characteristics, water depth, and interactions with the environment are only a few factors that influence how they behave dynamically[11,12]. Figure 1 shows the dynamics of water waves. The wavelength of a water wave, represented by the symbol λ, is the separation between two successive wave crests (or troughs). It symbolises the wave's spatial period, or the length of time the wave repeats its shape. A wave's wavelength in water is determined by a number of variables, such as the wave's frequency and depth. The connection between wavelength (λ), wave speed (c), and wave period (T) in deep water, when the depth is much higher than the wavelength, may be explained by $\lambda = c/f$. The amplitude of a water wave, represented by y. The amplitude of the water wave is measured vertically from the undisturbed water level (the equilibrium position) to the peak of the wave crest or the lowest point of the wave trough.

Nonlinear fractional differential equations have attracted a lot of attention lately. It significantly impacts how fractional calculus theory changes, and these forms are used in physics, engineering, and biology, among other domains[13]. Traveling wave solutions of nonlinear partial differential equations must be investigated to distinguish between various nonlinear situations in applied research and engineering. Only a few of the many nonlinear wave techniques that have been used in the past to illustrate various physics issues include heat flow, shallow water waves, wave propagation, optical fibers, plasma physics, fluid mechanics, biology, electricity, chemical kinematics, and quantum theory[14–18]. Thus, to investigate these substances, scores of effective strategies have been recommended in the circulated works by scholars, namely the improved modified extended tanh-function method[4], the (G′/G,1/G)-expansion technique[19,20], the modified extended tanh-function method[1,9,21], the $(G^{'}/G^2)$-expansion technique[22,23], the advanced $\exp(-\varnothing(\xi))$-expansion method[24–26], the tanh-coth method[27], the variational iteration method[28–30], the method of characteristics[31], the multiple Exp-function method[32–34], the sine-Gordon expansion method[3,35,36], rational sine-Gordon expansion method[37,38], Backlund transformations[39], ultraspherical wavelets collocation method[40], extended direct algebraic method[41], the unified method[42], the hyperbolic trigonometric method[43], the new auxiliary equation method[5], transformed rational function method[44], the Hirota bilinear method[45–47], the generalized Hirota bilinear method[48], Soret and Dufour effects[49], the rational $\tan(K(\rho))$-expansion technique[50], the improved $\tan(\Phi(\rho)/2)$-expansion technique[51], the binary Hirota polynomial scheme[52], the Kudryashov method[53], etc.

The remainder of the paper is organized as follows. In Sect. "Algorithm of the RSGE method", a basic description of the RSGE method is given. The mathematical formulation of the phi-four and CBS equations and their application using the RSGE approach are provided in Sect. "Application of the RSGE method". Graphical depictions of the solutions discovered are given in Sect. "Result and Discussion". The conclusions are presented in Sect. "Conclusion".

Algorithm of the RSGE method

The consistent fractional form $u(x,t) = U(\psi)$ with $\psi = a\left(x - \frac{vt^{\alpha}}{\alpha}\right)$ The unadventurous wave renovation[3,54–56] decreases the fractional Sine-Gordon equation in one dimension of the form.

$$\frac{\partial^2 u}{\partial x^2} - D_t^{2\alpha} u = m^2 \sin u, m\, is\, constant. \tag{5}$$

To the ODE

$$\frac{d^2 U}{d\psi^2} = \frac{m^2}{a^2\left(1 - v^2\right)} \sin U, \tag{6}$$

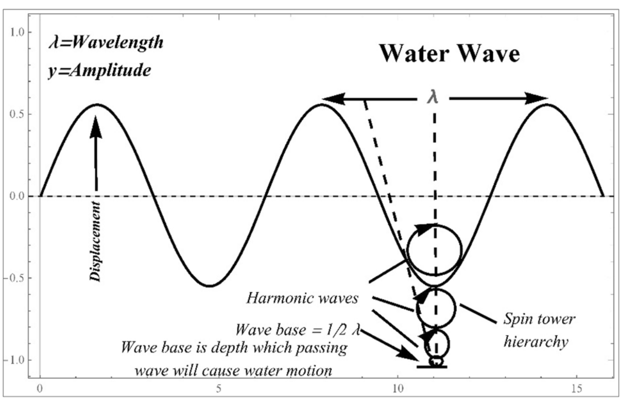

Figure 1. Dynamics of water waves.

where v indicates the velocity of the traveling wave illustrated in the transform[57]. Some simplifications lead

$$\left(\frac{d\left(\frac{U}{2}\right)}{d\psi}\right)^2 = \frac{m^2}{a^2\left(1-v^2\right)}\sin^2\frac{U}{2} + C, \tag{7}$$

where C is an integrating constant and is supposed to be zero for simplicity. Let $w(\psi) = \frac{U(\psi)}{2}$ and $b^2 = \frac{m^2}{a^2(1-v^2)}$. Then (7) is converted to

$$\frac{d(w)}{d\psi} = b\sin w. \tag{8}$$

Set $b = 1$ in (8). Then (8) yields two significant relations.

$$\sin w(\psi) = \left.\frac{2de^{\psi}}{d^2e^{2\psi}+1}\right|_{d=1} = \mathrm{sech}\psi, \tag{9}$$

or

$$\cos w(\psi) = \left.\frac{d^2e^{2\psi}-1}{d^2e^{2\psi}+1}\right|_{d=1} = \tanh\psi, \tag{10}$$

where d is a nonzero integrating constant. Then the fractional PDE of the form

$$P\left(u, D_t^{\alpha}u, u_x, D_{tt}^{2\alpha}, u_{xx}, \ldots\ldots\right) = 0, \tag{11}$$

can be reduced to an ODE

$$\widetilde{P} = \left(U, U\prime, U'', \ldots\ldots\right) = 0, \tag{12}$$

by using an equivalent wave transform $u(x,t) = U(\psi)$ where the transform variable ψ is specified as $a\left(x - \frac{vt^{\alpha}}{\alpha}\right)$. Then, the expected solution (12) of the form

$$U(\psi) = A_0 + \sum_{i=1}^{s} \tanh^{i-1}(\psi)(B_i\,\mathrm{sech}\,\psi + A_i\tanh\psi), \tag{13}$$

can be written as

$$U(w) = A_0 + \sum_{i=1}^{s} \cos^{i-1}(w)(B_i\sin w + A_i\cos w). \tag{14}$$

use Eqs. (9) and (10), Eq. (13) is a bivariate polynomial function in $\tanh\psi$ and $\mathrm{sech}\psi$, as is evident. Due to the relationships $\tanh^2\psi + \mathrm{sech}^2\psi = 1$, it is essential to note that this polynomial must be linear in one of these auxiliary functions. In this case, $\mathrm{sech}\psi$. We can now see that a subset of rational functions comprises polynomial functions. As a result, the latter is often far superior to the former in tasks like interpolation or approximating functions[58]. It is simple to assume that the same will hold while attempting to solve nonlinear evolution equations. The concept of rational expansion has been utilized in the literature before, but only in the context of one auxiliary function[58–60]. In this study, we propose expanding this concept to two additional tasks.

$$U(\psi) = \frac{\sum_{i=1}^{N}\tanh^{i-1}\psi(a_i\,\mathrm{sech}\,\psi + c_i\tanh\psi + a_0)}{\sum_{i=1}^{N}\tanh^{i-1}\psi(b_i\,\mathrm{sech}\,\psi + d_i\tanh\psi + b_0)}, \tag{15}$$

in place of Eq. (13), which can also be written as

$$U(\mathrm{w}) = \frac{\sum_{i=1}^{N}\cos^{i-1}\mathrm{w}(a_i\sin\mathrm{w} + c_i\cos\mathrm{w} + a_0)}{\sum_{i=1}^{N}\cos^{i-1}\mathrm{w}(b_i\sin\mathrm{w} + d_i\cos\mathrm{w} + b_0)}, \tag{16}$$

owing to (15)–(16). Setting up index limits with a uniform balance of the conditions in (12) is the first step in the procedure. The projected solution (15), engaging in (12), is replaced, and the coefficient of powers of sin and cos is assumed to be zero. Next, the coefficients are explained by the ensuing algebraic system. $a_0, a_1, b_0, b_1, \ldots\ldots$... If there are any answers, they are put together using (9)–(10) and ψ.

Application of the RSGE method

Application for the Phi-four equation

Employing the subsequent traveling wave transformation

$$\mathrm{u(x,t)} = \mathrm{U}(\psi), \text{where } \psi = \mathrm{q}x - p\frac{t^{\theta}}{\theta}.$$

on Eq. (4), we get

$$\left(p^2-q^2\right)U^{''}+\lambda^2U+\mu U^3=0, \tag{17}$$

With the asset of standardized balancing of the highest order derivative term $U^{''}$ and nonlinear term U^3 in Eq. 17, we find that $N=1$. Therefore, the auxiliary solution becomes:

$$\begin{aligned}
&\mu a_0^3+3\mu a_0a_1^2+\lambda^2a_0b_0^2-p^2a_1b_0b_1+q^2a_1b_0b_1+2\lambda^2a_1b_0b_1-p^2a_0b_1^2+q^2a_0b_1^2+\lambda^2a_0b_1^2\\
&-2p^2b_0c_1d_1+2q^2b_0c_1d_1+2p^2a_0d_1^2-2q^2a_0d_1^2=0,\\
&3\mu a_0^2c_1+3\mu a_1^2c_1-2p^2b_0^2c_1+2q^2b_0^2c_1+\lambda^2b_0^2c_1+p^2b_1^2c_1-q^2b_1^2c_1+\lambda^2b_1^2c_1+2p^2a_0b_0d_1\\
&-2q^2a_0b_0d_1+2\lambda^2a_0b_0d_1-p^2a_1b_1d_1+q^2a_1b_1d_1+2\lambda^2a_1b_1d_1=0,\\
&-3\mu a_0a_1^2+p^2a_1b_0b_1-q^2a_1b_0b_1-2\lambda^2a_1b_0b_1+3p^2a_0b_1^2-3q^2a_0b_1^2-\lambda^2a_0b_1^2+3\mu a_0c_1^2\\
&+2p^2b_0c_1d_1-2q^2b_0c_1d_1+2\lambda^2b_0c_1d_1-2p^2a_0d_1^2+2q^2a_0d_1^2+\lambda^2a_0d_1^2=0,\\
&-3\mu a_1^2c_1+2p^2b_0^2c_1-2q^2b_0^2c_1-p^2b_1^2c_1+q^2b_1^2c_1-\lambda^2b_1^2c_1+\mu c_1^3-2p^2a_0b_0d_1+2q^2a_0b_0d_1\\
&+p^2a_1b_1d_1-q^2a_1b_1d_1-2\lambda^2a_1b_1d_1+\lambda^2c_1d_1^2=0,\\
&-2p^2a_0b_1^2+2q^2a_0b_1^2=0,\\
&\mu a_0^3+3\mu a_0a_1^2+\lambda^2a_0b_0^2-p^2a_1b_0b_1+q^2a_1b_0b_1+2\lambda^2a_1b_0b_1-p^2a_0b_1^2+q^2a_0b_1^2+\lambda^2a_0b_1^2\\
&-2p^2b_0c_1d_1+2q^2b_0c_1d_1+2p^2a_0d_1^2-2q^2a_0d_1^2=0,\\
&3\mu a_0^2a_1+\mu a_1^3-p^2a_1b_0^2+q^2a_1b_0^2+\lambda^2a_1b_0^2-p^2a_0b_0b_1+q^2a_0b_0b_1+2\lambda^2a_0b_0b_1+\lambda^2a_1b_1^2\\
&-2p^2b_1c_1d_1+2q^2b_1c_1d_1+2p^2a_1d_1^2-2q^2a_1d_1^2=0,\\
&6\mu a_0a_1c_1-p^2b_0b_1c_1+q^2b_0b_1c_1+2\lambda^2b_0b_1c_1+2p^2a_1b_0d_1-2q^2a_1b_0d_1+2\lambda^2a_1b_0d_1\\
&-3p^2a_0b_1d_1+3q^2a_0b_1d_1+2\lambda^2a_0b_1d_1=0,\\
&-\mu a_1^3+2p^2a_1b_0^2-2q^2a_1b_0^2-\lambda^2a_1b_1^2+3\mu a_1c_1^2+p^2b_1c_1d_1-q^2b_1c_1d_1+2\lambda^2b_1c_1d_1\\
&-p^2a_1d_1^2+q^2a_1d_1^2+\lambda^2a_1d_1^2=0,\\
&2p^2a_0b_1d_1-2q^2a_0b_1d_1=0.
\end{aligned} \tag{18}$$

Solving the SAE Eq. (18) for q, A_0, A_1, B_1 we get several solutions sets as follows:

$$q=-\sqrt{p^2-2\lambda^2},a_0=0,a_1=\pm\frac{\sqrt{\lambda^2b_0^2-\lambda^2b_1^2}}{\sqrt{\mu}},c_1=\pm\frac{i\lambda b_0}{\sqrt{\mu}},d_1=0.$$

$$q=\sqrt{p^2-2\lambda^2},a_0=0,a_1=\pm\frac{\sqrt{\lambda^2b_0^2-\lambda^2b_1^2}}{\sqrt{\mu}},c_1=\pm\frac{i\lambda b_0}{\sqrt{\mu}},d_1=0.$$

$$q=-\sqrt{p^2-2\lambda^2},a_0=\pm\frac{i\lambda d_1}{\sqrt{\mu}},a_1=\pm\frac{\sqrt{\lambda^2b_0^2-\lambda^2d_1^2}}{\sqrt{\mu}},b_1=0,c_1=\pm\frac{i\lambda b_0}{\sqrt{\mu}}.$$

$$q=\sqrt{p^2-2\lambda^2},a_0=\pm\frac{i\lambda d_1}{\sqrt{\mu}},a_1=\pm\frac{\sqrt{\lambda^2b_0^2-\lambda^2d_1^2}}{\sqrt{\mu}},b_1=0,c_1=\pm\frac{i\lambda b_0}{\sqrt{\mu}}.$$

$$q=-\frac{\sqrt{2p^2-\lambda^2}}{\sqrt{2}},a_0=-\frac{i\lambda d_1}{\sqrt{\mu}},a_1=0,b_1=0,c_1=-\frac{i\lambda b_0}{\sqrt{\mu}}.$$

$$q=-\frac{\sqrt{2p^2-\lambda^2}}{\sqrt{2}},a_0=\frac{i\lambda d_1}{\sqrt{\mu}},a_1=0,b_1=0,c_1=\frac{i\lambda b_0}{\sqrt{\mu}}.$$

$$q=\frac{\sqrt{2p^2-\lambda^2}}{\sqrt{2}},a_0=-\frac{i\lambda d_1}{\sqrt{\mu}},a_1=0,b_1=0,c_1=-\frac{i\lambda b_0}{\sqrt{\mu}}.$$

$$q=\frac{\sqrt{2p^2-\lambda^2}}{\sqrt{2}},a_0=\frac{i\lambda d_1}{\sqrt{\mu}},a_1=0,b_1=0,c_1=\frac{i\lambda b_0}{\sqrt{\mu}}.$$

$$q=-\sqrt{p^2+\lambda^2},a_0=0,a_1=\pm\frac{\sqrt{2}\sqrt{-\lambda^2b_0^2+\lambda^2d_1^2}}{\sqrt{\mu}},b_1=0,c_1=0.$$

$$q=\sqrt{p^2+\lambda^2},a_0=0,a_1=\pm\frac{\sqrt{2}\sqrt{-\lambda^2b_0^2+\lambda^2d_1^2}}{\sqrt{\mu}},b_1=0,c_1=0.$$

$$q=-\sqrt{p^2-2\lambda^2}, a_0=0, a_1=0, b_0=\pm b_1, c_1=\pm\frac{i\lambda b_1}{\sqrt{\mu}}, d_1=0.$$

$$q=\sqrt{p^2-2\lambda^2}, a_0=0, a_1=0, b_0=\pm b_1, c_1=\pm\frac{i\lambda b_1}{\sqrt{\mu}}, d_1=0.$$

$$q=-\sqrt{p^2-2\lambda^2}, a_0=\pm\frac{i\lambda d_1}{\sqrt{\mu}}, a_1=\pm\frac{i\lambda d_1}{\sqrt{\mu}}, b_0=0, b_1=0, c_1=0.$$

$$q=-\sqrt{p^2-2\lambda^2}, a_0=0, a_1=\pm\frac{\lambda b_0}{\sqrt{\mu}}, b_1=0, c_1=\pm\frac{i\lambda b_0}{\sqrt{\mu}}, d_1=0.$$

$$q=\sqrt{p^2-2\lambda^2}, a_0=\pm\frac{i\lambda d_1}{\sqrt{\mu}}, a_1=\pm\frac{i\lambda d_1}{\sqrt{\mu}}, b_0=0, b_1=0, c_1=0.$$

$$q=\sqrt{p^2-2\lambda^2}, a_0=0, a_1=\pm\frac{\lambda b_0}{\sqrt{\mu}}, b_1=0, c_1=\pm\frac{i\lambda b_0}{\sqrt{\mu}}, d_1=0.$$

$$q=\pm\frac{\sqrt{2p^2-\lambda^2}}{\sqrt{2}}, a_0=0, a_1=0, b_1=0, c_1=\pm\frac{i\lambda b_0}{\sqrt{\mu}}, d_1=0.$$

$$q=-\sqrt{p^2+\lambda^2}, a_0=0, a_1=\pm\frac{\sqrt{2}\lambda d_1}{\sqrt{\mu}}, b_0=0, b_1=0, c_1=0.$$

$$q=-\sqrt{p^2+\lambda^2}, a_0=0, a_1=\pm\frac{i\lambda d_1}{\sqrt{\mu}}, b_0=\pm\sqrt{\frac{3}{2}}d_1, b_1=0, c_1=0.$$

$$q=-\sqrt{p^2+\lambda^2}, a_0=0, a_1=\pm\frac{i\sqrt{2}\lambda d_1}{\sqrt{\mu}}, b_0=-\sqrt{2}d_1, b_1=0, c_1=0.$$

$$q=-\sqrt{p^2+\lambda^2}, a_0=0, a_1=\pm\frac{i\sqrt{2}\lambda d_1}{\sqrt{\mu}}, b_0=\sqrt{2}d_1, b_1=0, c_1=0.$$

$$q=-\sqrt{p^2+\lambda^2}, a_0=0, a_1=\pm\frac{i\sqrt{2}\lambda b_0}{\sqrt{\mu}}, b_1=0, c_1=0, d_1=0.$$

$$q=\sqrt{p^2+\lambda^2}, a_0=0, a_1=\pm\frac{\sqrt{2}\lambda d_1}{\sqrt{\mu}}, b_0=0, b_1=0, c_1=0.$$

$$q=\sqrt{p^2+\lambda^2}, a_0=0, a_1=\pm\frac{i\lambda d_1}{\sqrt{\mu}}, b_0=\pm\sqrt{\frac{3}{2}}d_1, b_1=0, c_1=0.$$

$$q=\sqrt{p^2+\lambda^2}, a_0=0, a_1=\pm\frac{i\sqrt{2}\lambda d_1}{\sqrt{\mu}}, b_0=\pm\sqrt{2}d_1, b_1=0, c_1=0.$$

$$q=\sqrt{p^2+\lambda^2}, a_0=0, a_1=\pm\frac{i\sqrt{2}\lambda b_0}{\sqrt{\mu}}, b_1=0, c_1=0, d_1=0.$$

We obtained the precise Eq. (4) solutions concerning these solution sets.

$$U_{1,2,3,4}(x,t)=\pm\frac{i\lambda\mathrm{Sinh}[\psi]b_0\pm\sqrt{\lambda^2\left(b_0^2-b_1^2\right)}}{\sqrt{\mu}(\mathrm{Cosh}[\psi]b_0+b_1)};\ \psi=-\frac{pt^\theta}{\theta}-x\sqrt{p^2-2\lambda^2}.$$

$$U_{5,6,7,8}(x,t)=\pm\frac{i\lambda\mathrm{Sinh}[\psi]b_0\pm\sqrt{\lambda^2\left(b_0^2-b_1^2\right)}}{\sqrt{\mu}(\mathrm{Cosh}[\psi]b_0+b_1)};\ \psi=-\frac{pt^\theta}{\theta}+x\sqrt{p^2-2\lambda^2}.$$

$$U_{9,10,11,12}(x,t)=\pm\frac{i\lambda d_1\pm\mathrm{Sech}[\psi]\sqrt{\lambda^2(b_0^2-d_1^2)}+i\lambda b_0\mathrm{Tanh}[\psi]}{\sqrt{\mu}(b_0+d_1\mathrm{Tanh}[\psi])};\ \psi=-\frac{pt^\theta}{\theta}-x\sqrt{p^2-2\lambda^2}.$$

$$U_{13,14,15,16}(x,t)=\pm\frac{i\lambda d_1\pm\mathrm{Sech}[\psi]\sqrt{\lambda^2(b_0^2-d_1^2)}+i\lambda b_0\mathrm{Tanh}[\psi]}{\sqrt{\mu}(b_0+d_1\mathrm{Tanh}[\psi])};\ \psi=-\frac{pt^\theta}{\theta}+x\sqrt{p^2-2\lambda^2}.$$

$$U_{17,18}(x,t)=\pm\frac{i\lambda(d_1+b_0\mathrm{Tanh}[\psi])}{\sqrt{\mu}(b_0+d_1\mathrm{Tanh}[\psi])};\ \psi=-\frac{pt^\theta}{\theta}-\frac{x\sqrt{2p^2-\lambda^2}}{\sqrt{2}}.$$

$$U_{19,20}(x,t)=\pm\frac{\sqrt{2}\mathrm{Sech}[\psi]\sqrt{-\lambda^2\left(b_0^2-d_1^2\right)}}{\sqrt{\mu}(b_0+d_1\mathrm{Tanh}[\psi])};\ \psi=-\frac{pt^\theta}{\theta}-x\sqrt{p^2+\lambda^2}.$$

$$U_{21,22}(x,t)=\pm\frac{\sqrt{2}\mathrm{Sech}[\psi]\sqrt{-\lambda^2\left(b_0^2-d_1^2\right)}}{\sqrt{\mu}(b_0+d_1\mathrm{Tanh}[\psi])};\ \psi=-\frac{pt^\theta}{\theta}+x\sqrt{p^2+\lambda^2}.$$

$$U_{23,24}(x,t)=\pm\frac{i\lambda\mathrm{Coth}\left[\frac{\psi}{2}\right]}{\sqrt{\mu}};\ \psi=-\frac{pt^\theta}{\theta}-x\sqrt{p^2-2\lambda^2}.$$

$$U_{25,26}(x,t)=\pm\frac{i\lambda\mathrm{Tanh}\left[\frac{\psi}{2}\right]}{\sqrt{\mu}};\ \psi=-\frac{pt^\theta}{\theta}-x\sqrt{p^2-2\lambda^2}.$$

$$U_{27,28}(x,t)=\pm\frac{i\lambda\mathrm{Coth}\left[\frac{\psi}{2}\right]}{\sqrt{\mu}};\ \psi=-\frac{pt^\theta}{\theta}+x\sqrt{p^2-2\lambda^2}.$$

$$U_{29,30}(x,t)=\pm\frac{i\lambda\mathrm{Tanh}\left[\frac{\psi}{2}\right]}{\sqrt{\mu}};\ \psi=-\frac{pt^\theta}{\theta}+x\sqrt{p^2-2\lambda^2}.$$

$$U_{31,32,33,34}(x,t)=\pm\frac{\lambda(\mathrm{Sech}[\psi]\pm i\mathrm{Tanh}[\psi])}{\sqrt{\mu}};\ \psi=-\frac{pt^\theta}{\theta}-x\sqrt{p^2-2\lambda^2}.$$

$$U_{35,36}(x,t)=\pm\frac{i\lambda\mathrm{Tanh}[\psi]}{\sqrt{\mu}};\ \psi=-\frac{pt^\theta}{\theta}-\frac{x\sqrt{2p^2-\lambda^2}}{\sqrt{2}}.$$

$$U_{37,38}(x,t)=\pm\frac{i\lambda\mathrm{Tanh}[\psi]}{\sqrt{\mu}};\ \psi=-\frac{pt^\theta}{\theta}+\frac{x\sqrt{2p^2-\lambda^2}}{\sqrt{2}}.$$

$$U_{39,40}(x,t)=\pm\frac{\sqrt{2}\lambda\mathrm{Csch}[\psi]}{\sqrt{\mu}};\ \psi=-\frac{pt^\theta}{\theta}-x\sqrt{p^2+\lambda^2}.$$

$$U_{41,42,43,44}(x,t)=\pm\frac{2i\lambda\mathrm{Sech}[\psi]}{\sqrt{\mu}(\sqrt{6}\pm2\mathrm{Tanh}[\psi])};\ \psi=-\frac{pt^\theta}{\theta}-x\sqrt{p^2+\lambda^2}.$$

$$U_{45,46,47,48}(x,t)=\pm\frac{2i\lambda\mathrm{Sech}[\psi]}{\sqrt{\mu}(\sqrt{6}\pm2\mathrm{Tanh}[\psi])};\ \psi=-\frac{pt^\theta}{\theta}+x\sqrt{p^2+\lambda^2}.$$

$$U_{49,50}(x,t)=\pm\frac{i\sqrt{2}\lambda\mathrm{Sech}[\psi]}{\sqrt{\mu}(\sqrt{2}-\mathrm{Tanh}[\psi])};\ \psi=-\frac{pt^{\theta}}{\theta}-x\sqrt{p^2+\lambda^2}.$$

$$U_{51,52}(x,t)=\pm\frac{i\sqrt{2}\lambda\mathrm{Sech}[\psi]}{\sqrt{\mu}(\sqrt{2}+\mathrm{Tanh}[\psi])};\ \psi=-\frac{pt^{\theta}}{\theta}+x\sqrt{p^2+\lambda^2}.$$

$$U_{53,54}(x,t)=\pm\frac{i\sqrt{2}\lambda\mathrm{Sech}[\psi]}{\sqrt{\mu}(\sqrt{2}+\mathrm{Tanh}[\psi])};\ \psi=-\frac{pt^{\theta}}{\theta}-x\sqrt{p^2+\lambda^2}.$$

$$U_{55,56}(x,t)=\pm\frac{i\sqrt{2}\lambda\mathrm{Sech}[\psi]}{\sqrt{\mu}};\ \psi=-\frac{pt^{\theta}}{\theta}-x\sqrt{p^2+\lambda^2}.$$

$$U_{57,58}(x,t)=\pm\frac{i\sqrt{2}\lambda\mathrm{Sech}[\psi]}{\sqrt{\mu}};\ \psi=-\frac{pt^{\theta}}{\theta}+x\sqrt{p^2+\lambda^2}.$$

$$U_{59,60}(x,t)=\pm\frac{\sqrt{2}\lambda\mathrm{Csch}[\psi]}{\sqrt{\mu}};\ \psi=-\frac{pt^{\theta}}{\theta}+x\sqrt{p^2+\lambda^2}.$$

Application for the (2 + 1)-dimensional CBS equation

Employing the subsequent traveling wave transformation

$$\mathrm{u}(\mathrm{x},\mathrm{y},\mathrm{t})=\mathrm{U}(\psi)\mathrm{and}\psi=\mathrm{x}+\mathrm{y}-\mathrm{p}\frac{\mathrm{t}^{\theta}}{\theta},\tag{19}$$

on Eq. (3), we get,

$$\mathrm{pU}'+\left(\frac{\lambda+\mu}{2}\right)\left(\mathrm{U}'\right)^2+\mathrm{U}'''=0,\tag{20}$$

With the asset of standardized balancing of the highest order derivative term U''' and nonlinear term $(U')^2$ in Eq. 20, we find that $N=1$. Therefore, the auxiliary solution becomes:

$$p=-1,a_1=\frac{a_0b_1}{b_0}+\frac{6b_1d_1}{(\lambda+\mu)b_0}\pm\frac{6\sqrt{(\lambda+\mu)^2d_1^4\left(-b_0^2+b_1^2+d_1^2\right)}}{(\lambda+\mu)^2d_1^2},c_1=\frac{-6b_0^2+\lambda a_0d_1+\mu a_0d_1+6d_1^2}{(\lambda+\mu)b_0}.$$

$$p=-1,a_0=-\frac{6d_1}{\lambda+\mu},a_1=\frac{(\lambda+\mu)^2b_1c_1d_1\pm6\sqrt{(\lambda+\mu)^2d_1^4\left(b_1^2+d_1^2\right)}}{(\lambda+\mu)^2d_1^2},b_0=0.$$

$$p=-1,a_1=\pm\frac{6\sqrt{-b_0^2+d_1^2}}{\sqrt{\lambda^2+2\lambda\mu+\mu^2}},b_1=0,c_1=\frac{-6b_0^2+\lambda a_0d_1+\mu a_0d_1+6d_1^2}{(\lambda+\mu)b_0}.$$

$$p=-4,a_1=0,b_1=0,c_1=\frac{-12b_0^2+\lambda a_0d_1+\mu a_0d_1+12d_1^2}{(\lambda+\mu)b_0}.$$

$$p=-1,a_1=\frac{(\lambda+\mu)^2a_0b_0b_1\pm6\sqrt{-(\lambda+\mu)^2b_0^4\left(b_0^2-b_1^2\right)}}{(\lambda+\mu)^2b_0^2},c_1=-\frac{6b_0}{\lambda+\mu},d_1=0.$$

$$p=-1,a_1=\frac{(\lambda a_0+\mu a_0-12b_0)b_1}{(\lambda+\mu)b_0},c_1=-a_0,d_1=-b_0.$$

$$p=-1,a_1=\frac{(\lambda a_0+\mu a_0+12b_0)b_1}{(\lambda+\mu)b_0},c_1=a_0,d_1=b_0.$$

$$p=-1,a_0=-\frac{6d_1}{\lambda+\mu},a_1=\pm\frac{6d_1}{\sqrt{\lambda^2+2\lambda\mu+\mu^2}},b_0=0,b_1=0.$$

$$p=-4, a_1=0, b_1=0, c_1=-\frac{12b_0}{\lambda+\mu}, d_1=0.$$

$$p=-1, a_1=-\frac{6b_0}{\sqrt{-\lambda^2-2\lambda\mu-\mu^2}}, b_1=0, c_1=-\frac{6b_0}{\lambda+\mu}, d_1=0.$$

$$p=-1, a_1=\frac{6b_0}{\sqrt{-\lambda^2-2\lambda\mu-\mu^2}}, b_1=0, c_1=\frac{6b_0}{\lambda+\mu}, d_1=0.$$

We obtained the precise Eq. (3) solutions concerning these solution sets.

$$U_{61,62}(x,y,t)=\frac{a_0}{b_0}-\frac{6\left((\lambda+\mu)\text{Sinh}[\psi]b_0^2d_1^2-(\lambda+\mu)d_1^3(b_1+\text{Sinh}[\psi]d_1)\pm b_0\sqrt{(\lambda+\mu)^2d_1^4\left(-b_0^2+b_1^2+d_1^2\right)}\right)}{(\lambda+\mu)^2b_0d_1^2(\text{Cosh}[\psi]b_0+b_1+\text{Sinh}[\psi]d_1)}; \psi=x+y+\frac{t^\theta}{\theta}.$$

$$U_{63,64}(x,y,t)=\frac{-6(\lambda+\mu)\text{Cosh}[\psi]d_1^3+(\lambda+\mu)^2c_1d_1(b_1+\text{Sinh}[\psi]d_1)\pm 6\sqrt{(\lambda+\mu)^2d_1^4(b_1^2+d_1^2)}}{(\lambda+\mu)^2d_1^2(b_1+\text{Sinh}[\psi]d_1)}; \psi=x+y+\frac{t^\theta}{\theta}.$$

$$U_{65,66}(x,y,t)=\frac{a_0\pm\frac{6\text{Sech}[\psi]\sqrt{-b_0^2+d_1^2}}{\sqrt{(\lambda+\mu)^2}}+\frac{\left(-6b_0^2+d_1((\lambda+\mu)a_0+6d_1)\right)\text{Tanh}[\psi]}{(\lambda+\mu)b_0}}{b_0+d_1\text{Tanh}[\psi]}; \psi=x+y+\frac{t^\theta}{\theta}.$$

$$U_{67}(x,y,t)=\frac{a_0+\frac{12\left(-b_0^2+d_1^2\right)\text{Tanh}[\psi]}{(\lambda+\mu)(b_0+d_1\text{Tanh}[\psi])}}{b_0}; \psi=x+y+\frac{4t^\theta}{\theta}.$$

$$U_{68}(x,y,t)=\frac{a_0b_0-\frac{6\text{Sech}[\psi]\left((\lambda+\mu)\text{Sinh}[\psi]b_0^3+\sqrt{-(\lambda+\mu)^2b_0^4(b_0^2-b_1^2)}\right)}{(\lambda+\mu)^2(b_0+\text{Sech}[\psi]b_1)}}{b_0^2}; \psi=x+y+\frac{t^\theta}{\theta}.$$

$$U_{69}(x,y,t)=\frac{-6(\lambda+\mu)\text{Sinh}[\psi]b_0^3+(\lambda+\mu)^2a_0b_0(\text{Cosh}[\psi]b_0+b_1)+6\sqrt{-(\lambda+\mu)^2b_0^4(b_0^2-b_1^2)}}{(\lambda+\mu)^2b_0^2(\text{Cosh}[\psi]b_0+b_1)}; \psi=x+y+\frac{t^\theta}{\theta}.$$

$$U_{70}(x,y,t)=\frac{a_0}{b_0}-\frac{12\text{Sech}[\psi]b_1}{(\lambda+\mu)(\text{Sech}[\psi]b_1-b_0(-1+\text{Tanh}[\psi]))}; \psi=x+y+\frac{t^\theta}{\theta}.$$

$$U_{71}(x,y,t)=\frac{a_0}{b_0}+\frac{12b_1}{(\lambda+\mu)(e^\psi b_0+b_1)}; \psi=x+y+\frac{t^\theta}{\theta}.$$

$$U_{72,73}(x,y,t)=-\frac{6\text{Coth}[\psi]}{\lambda+\mu}\pm\frac{6\text{Csch}[\psi]}{\sqrt{(\lambda+\mu)^2}}+\frac{c_1}{d_1}; \psi=x+y+\frac{t^\theta}{\theta}.$$

$$U_{74}(x,y,t)=\frac{a_0}{b_0}-\frac{12\text{Tanh}[\psi]}{\lambda+\mu}; \psi=x+y+\frac{4t^\theta}{\theta}.$$

$$U_{75,76}(x,y,t)=\frac{6\text{Sech}[\psi]}{\sqrt{-(\lambda+\mu)^2}}+\frac{a_0}{b_0}\pm\frac{6\text{Tanh}[\psi]}{\lambda+\mu}; \psi=x+y+\frac{t^\theta}{\theta}.$$

Result and discussion

This section defines the recently discovered precise solutions to the time-fractional phi-four equation and the (2+1) dimensional CBS equation using physical and visual examples. The best way to illustrate every essential component of real-life events is through visualization. By selecting proper fractional values, we also used MATLAB's computational capabilities. We assessed its conventional features while charging various exorbitant fees for unknown factors. The detailed proofs for the equations are shown in Figs. 2, 3, 4, 5, 6, 7, 8, 9, 10, 11, 12, 13 and 14.

Graphical and physical explanation

A famous example of this wave is a traveling wave that forms on the surface of an ocean, lake, or river. Water waves have a particular behavior because of how gravity and surface tension forces interact to determine their

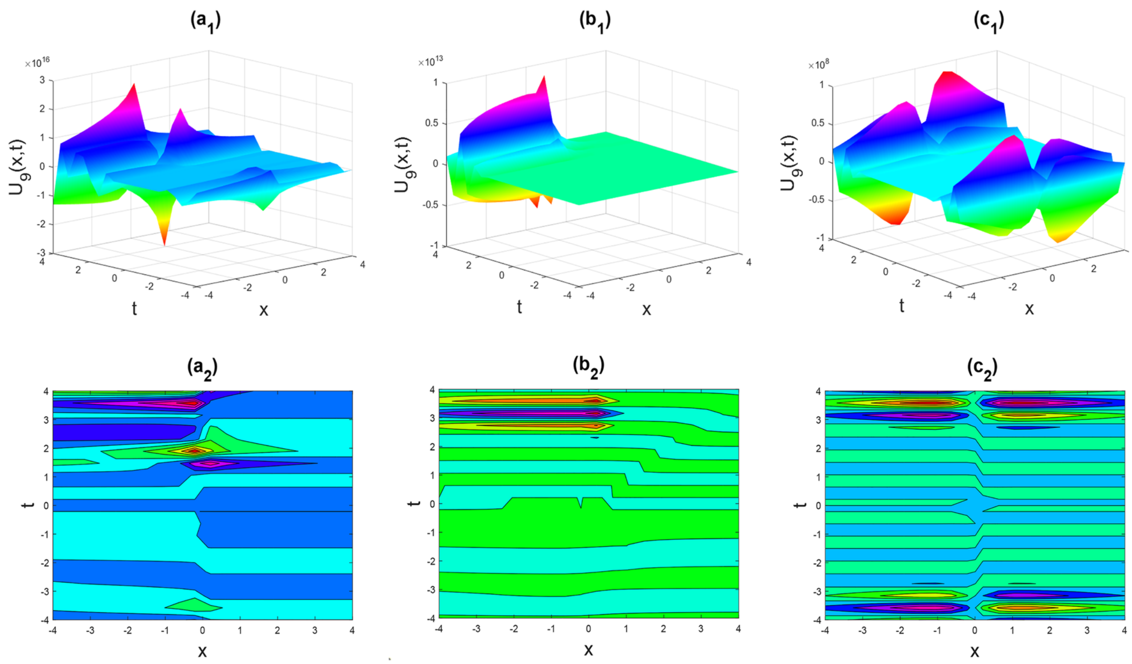

Figure 2. Kink-soliton shape of the imaginary part of $U_9(x, t)$ for the parameters $p = 0.5, b_0 = 1, d_1 = 0.1, \lambda = 1, \mu = 1, \theta = 0.3, 0.6, 1$.

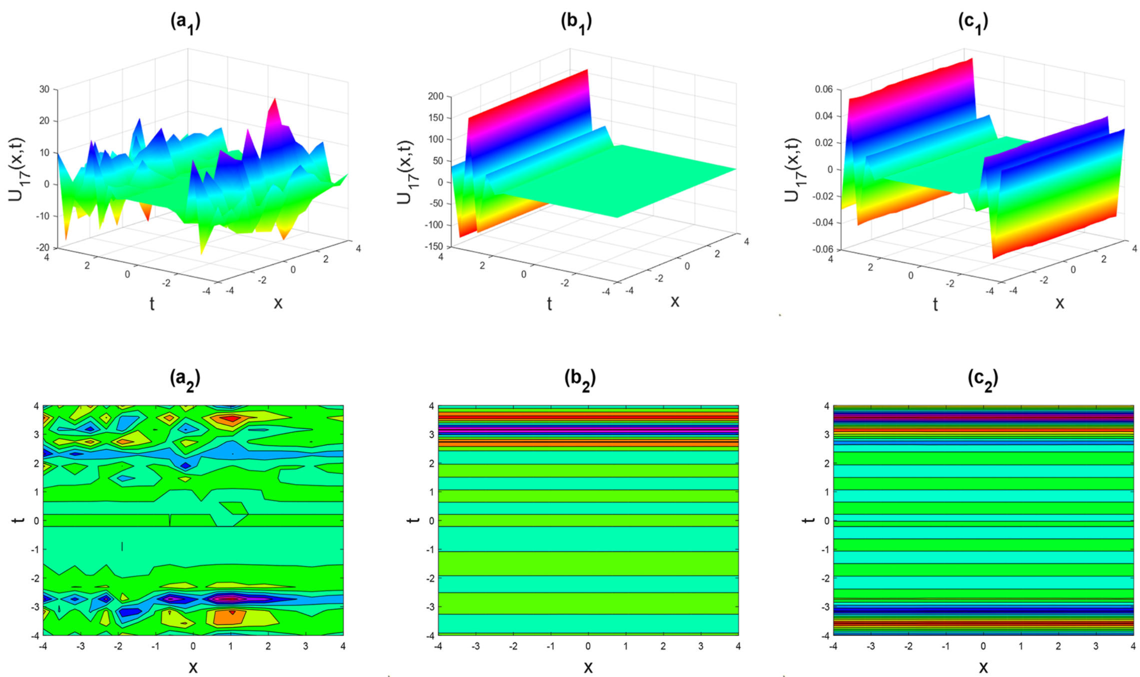

Figure 3. Kink-soliton shape of the real part of $U_{17}(x, t)$ for the parameters $p = 0.5, b_0 = 1, d_1 = 0.1, \lambda = 1, \mu = 1, \theta = 0.3, 0.6, 1$.

velocity. When the water's surface impedes, visualize a body of calm water at rest and experiencing moving waveforms. The wind blowing across the sea, dumping of an object, seismic activity, and other factors might all be factors in this disruption. Take pond ripples as an example, which are caused by the wind. Water molecules are drawn together at a body of water's surface by surface tension, which is a cohesive force. In addition, the force of gravity is pulling the water downward.

The interaction of these two forces results in a restoring force that tends to bring the water's surface back to its equilibrium position. A portion of the water molecules are forced to flow upward to form crests, which are recognized, and downward to produce troughs when the wind blows over the water, transferring energy to the surface. The disturbance propagates over the water's character due to oscillations brought on by the up-and-down

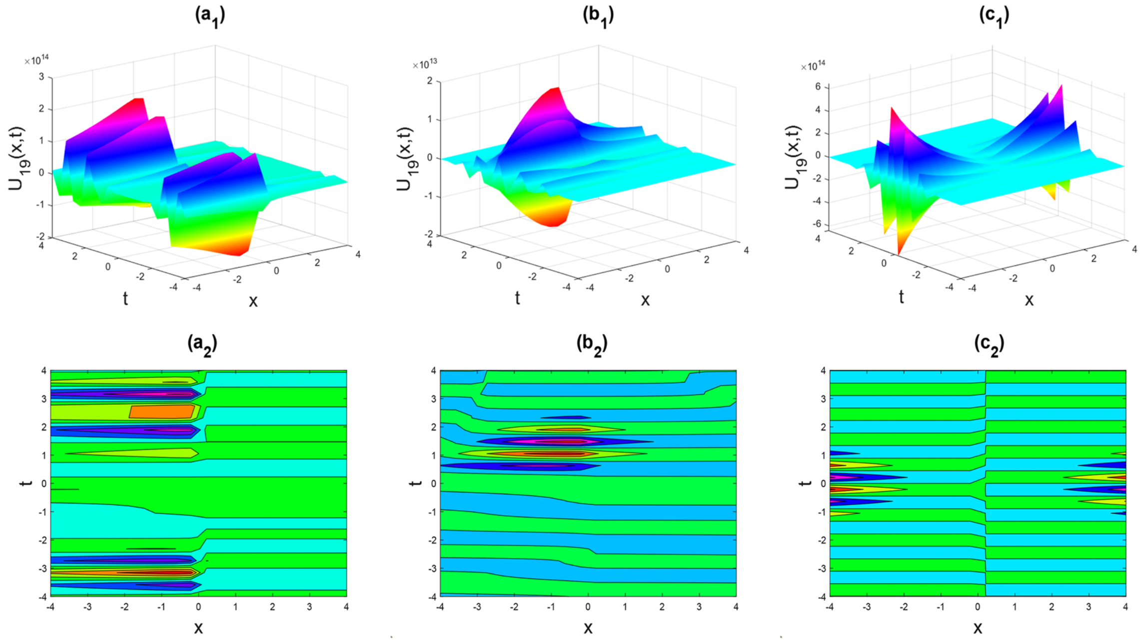

Figure 4. Kink shape of the imaginary part of $U_{19}(x,t)$ for the parameters $p=0.5, b_0=1, d_1=0.1, \lambda=1, \mu=1, \theta=0.3, 0.6, 1$.

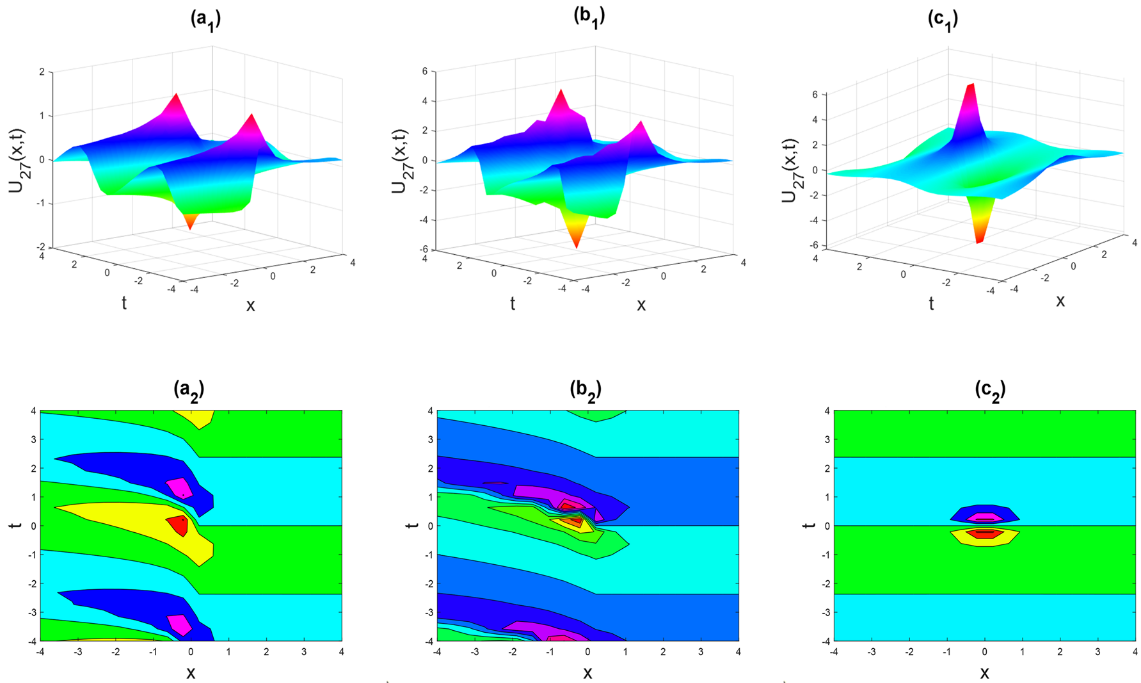

Figure 5. The rogue wave shape of the real part of $U_{27}(x,t)$ for the parameters $p=0.5, \lambda=1, \mu=1, \theta=0.3, 0.6, 1$.

motion of water molecules. When water molecules contact, they exchange energy and momentum. Gravity, surface tension, and a small amount of horizontal water molecule displacement work together to disperse these oscillations throughout the water. The wave's wavelength and the water's depth are two factors that influence how quickly a wave moves. The major influences on the wave speed of deep-water waves are the acceleration brought on by gravity and the water depth. The water wave's motion transfers energy from one place to another. The wave disperses the importance of the initial disturbance across the water's surface without displacing a large amount of water mass in the direction of propagation. Waves in water can interfere with one another and produce interference patterns. Dissipation is the term for this. Positive interference raises wave amplitudes, leading to more enormous waves than destructive interference, which can cause wave cancellation. As long-distance water waves travel through the water, friction, and viscosity eventually cause the waves to lose energy, which

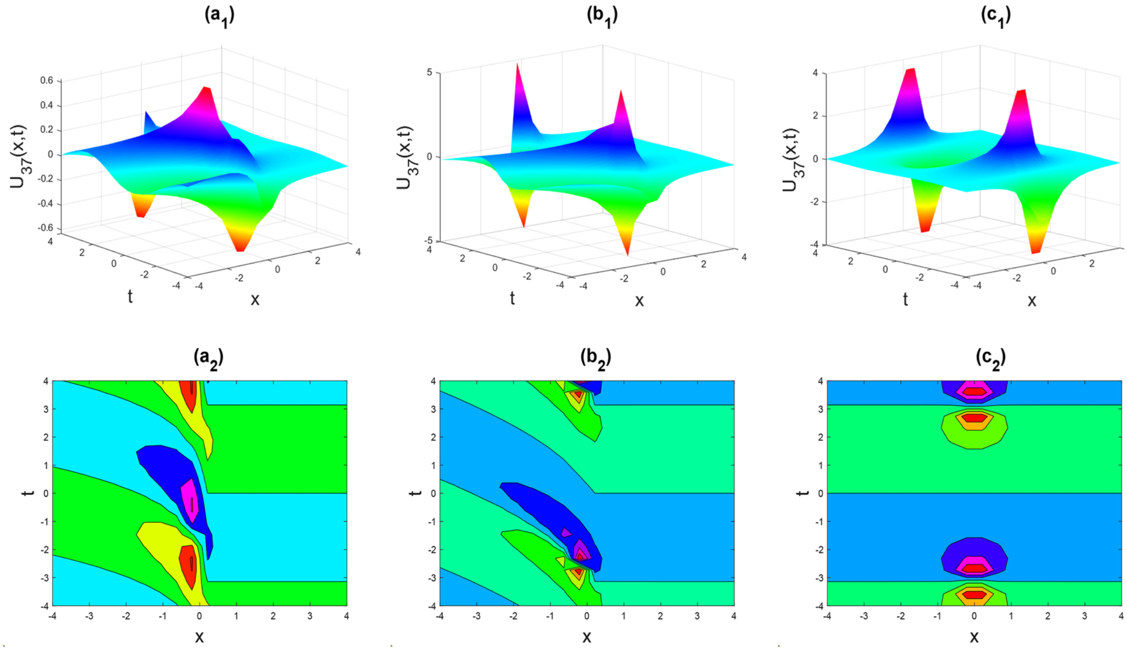

Figure 6. The rogue wave shape of the real part of $U_{37}(x,t)$ for the parameters $p = 0.5, \lambda = 1, \mu = 1, \theta = 0.3, 0.6, 1$.

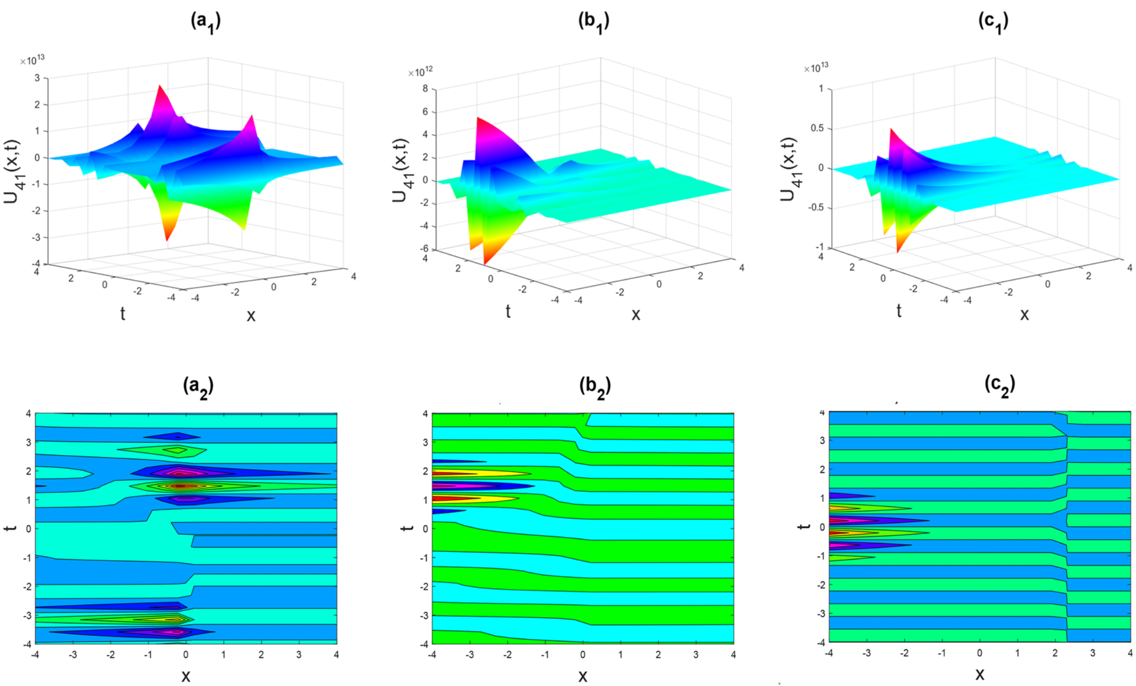

Figure 7. Kink shape of the imaginary part of $U_{41}(x,t)$ for the parameters $p = 0.5, \lambda = 1, \mu = 1, \theta = 0.3, 0.6, 1$.

leads to the waves dissipating. Coastal dynamics, marine transportation, and engineering all depend on water waves. Understanding the behavior of ocean waves is essential for predicting coastal erosion, building ships, and guaranteeing maritime safety.

Figures 2, 3, 4, 5, 6, 7, 8, 9, 10, 11, 12, 13 and 14 depict the many solution versions of the time-fractional phi-four and $(2+1)$ dimensional CBS equation. Each picture has two rows: the first row represents the 3D surface plot, while the second row represents the contour plot. Here, we presented the contour and 3D surface plots of many solutions. We have implemented some innovative solutions: Various shapes such as kink, multiple kink, rogue wave, soliton, lone soliton, multiple soliton, dark soliton, double soliton, and lump can be observed. The data have been altered for various values of θ, where θ ranges from 0.3 to 1. When the value of θ is changed from 0.3 to 1, the solution forms can transform solitary soliton shapes to multiple soliton shapes, from singular

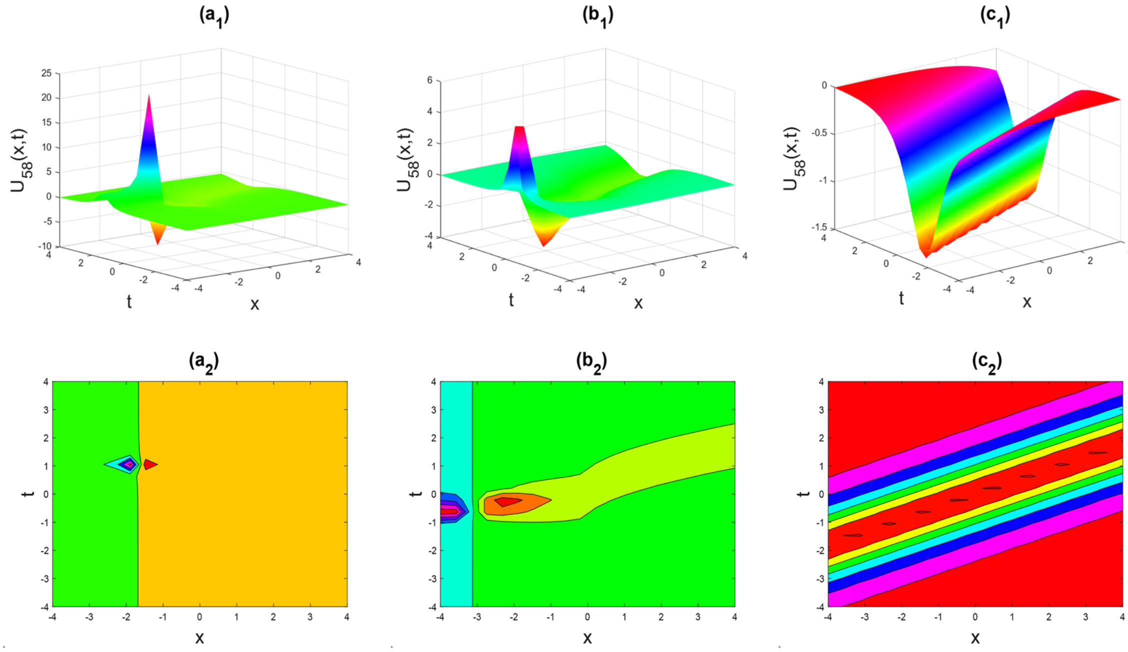

Figure 8. Soliton shape of the imaginary part of $U_{58}(x,t)$ for the parameters $p = 0.5, \lambda = 1, \mu = 1, \theta = 0.3, 0.6, 1$.

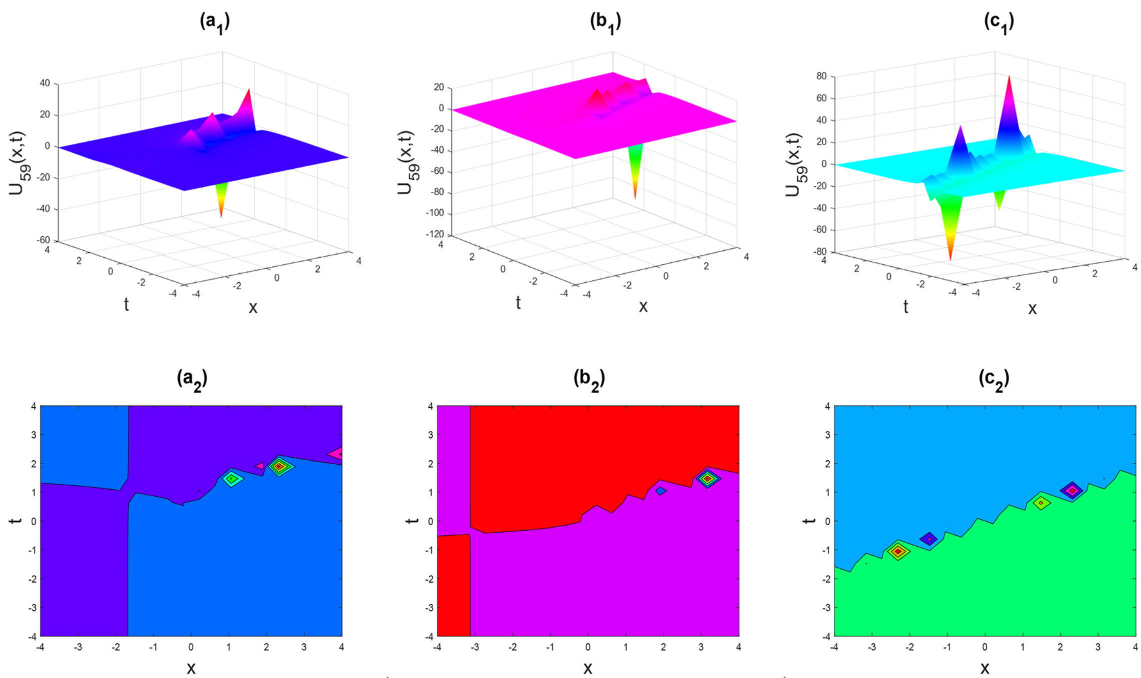

Figure 9. Soliton shape of the real part of $U_{59}(x,t)$ for the parameters $p = 0.5, \lambda = 1, \mu = 1, \theta = 0.3, 0.6, 1$.

kink-soliton shapes to multiple kink-soliton shapes, and from soliton shapes to dark soliton shapes, among others. The wave's nonlinearity induces temporal variations in its profile as it traverses the medium, but dispersion counteracts this effect, preventing the wave from diffusing or distorting. Overall, solitary waves are captivating occurrences that arise from the delicate equilibrium between dispersion and nonlinearity in a medium. These waves are crucial in several fields of physics and engineering due to their capacity to maintain their shape and propagate across long distances without dispersing or losing energy, owing to this state of equilibrium.

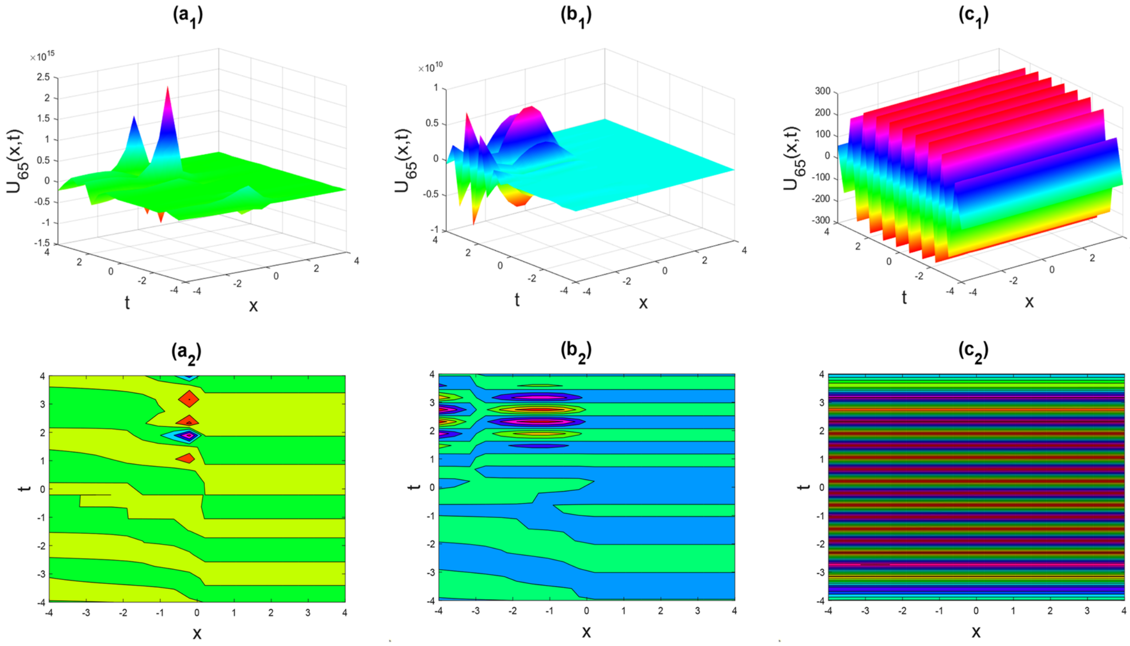

Figure 10. Multiple Kink-soliton shapes of the real part of $U_{65}(x, y, t)$ for the parameters $a_0 = 1, b_0 = 0.5, d_1 = -0.1, \lambda = 1, \mu = 1, y = 0, \theta = 0.3, 0.6, 1.$

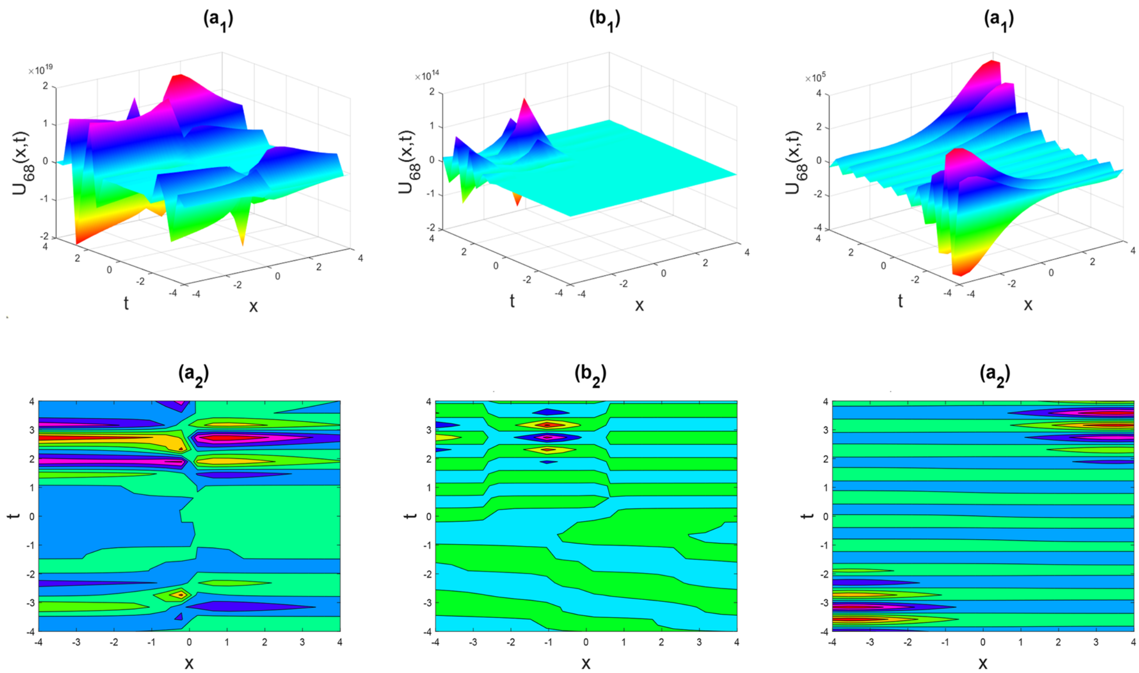

Figure 11. Multiple soliton shapes of the real part of $U_{68}(x, y, t)$ for the parameters $a_0 = 1, b_0 = 0.5, b_1 = -0.1, \lambda = 1, \mu = 1, y = 0, \theta = 0.3, 0.6, 1.$

Conclusion

The traveling wave solution for the time-fractional phi-four equation and the $(2+1)$ dimensional CBS equation was found using the rational sine-Gordon expansion approach. A tried-and-true technique is the rational sine-Gordon expansion to resolve nonlinear partial differential equations. When the wave profile is investigated for the created generic parametric values, many depicted solitons, rogue waves, singular kink, periodic, lump, and asymptotic type solitons may be found. These solitons were constructed utilizing exponential, hyperbolic, and trigonometric structures. We have mainly focused on the influence of the values or quantities of changes for

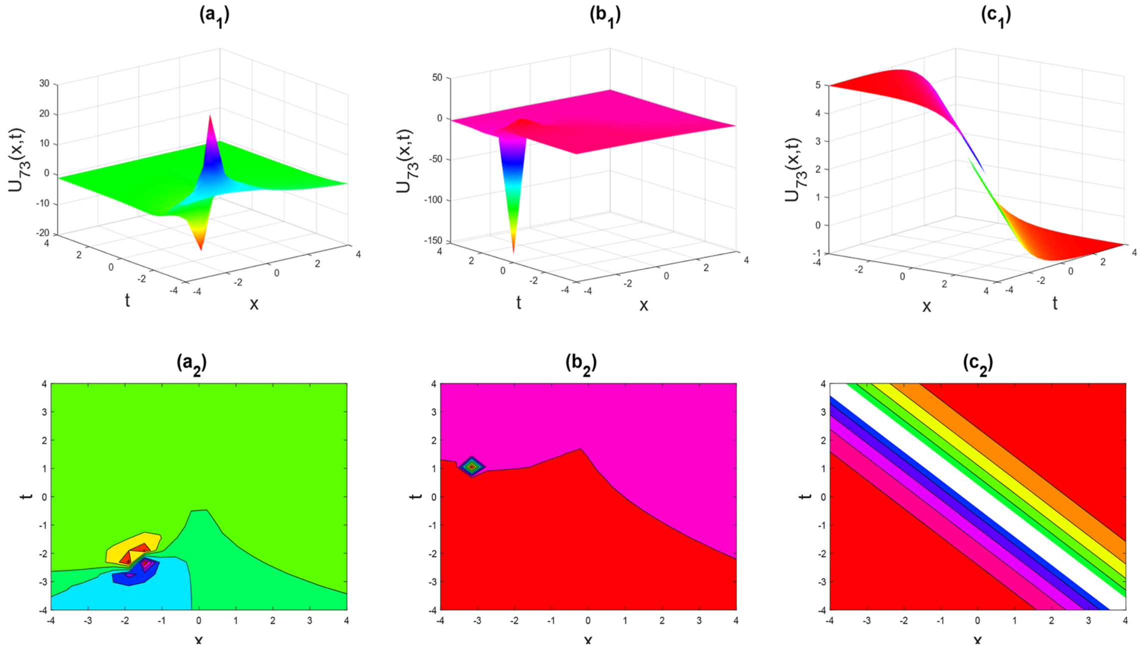

Figure 12. Kink-soliton shape of the real part of $U_{73}(x,y,t)$ for the parameters $c_1 = 1, d_1 = 0.5, \lambda = 1, \mu = 1, y = 0, \theta = 0.3, 0.6, 1.$

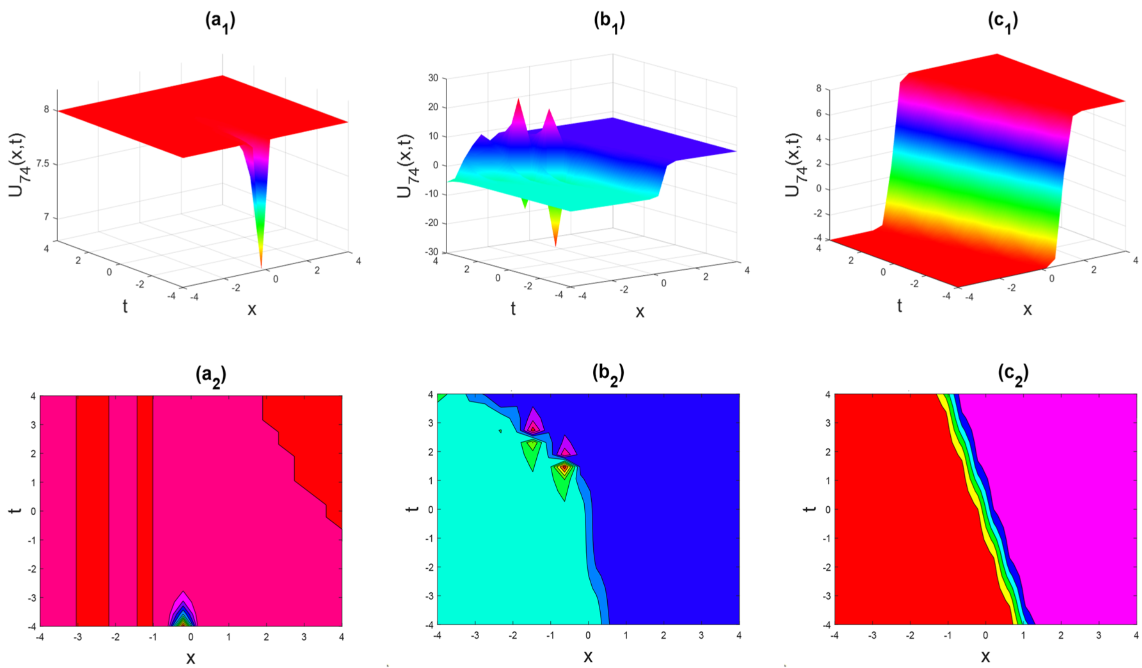

Figure 13. Kink-soliton shape of the real part of $U_{74}(x,y,t)$ for the parameters $a_0 = 1, b_0 = 0.5, \lambda = 1, \mu = 1, y = 0, \theta = 0.3, 0.6, 1.$

different values of one parameter (θ) on the dynamic behavior of the water waves. Exponential and trigonometric functions express the calculated solutions. The space–time fractional NLS +, NLS- and UNLS models from nonlinear optics, fluid mechanics, quantum theory, and other theoretical and numerical fields will be used to explain the physical significance of the traveling wave solutions in this work. This method may be used with complex nonlinear physics, engineering, and applied mathematics models. It is conceivable that certain types of nonlinear problems may not be solvable using this methodology. While it may not be capable of handling complex nonlinear systems, it is highly efficient in solving specific types of equations. Employ other methods to verify the obtained solutions, such as asymptotic analysis, numerical simulations, or, if accessible, comparison with empirical data. This enhances the reliability and accuracy of the generated solutions. Utilise the rational

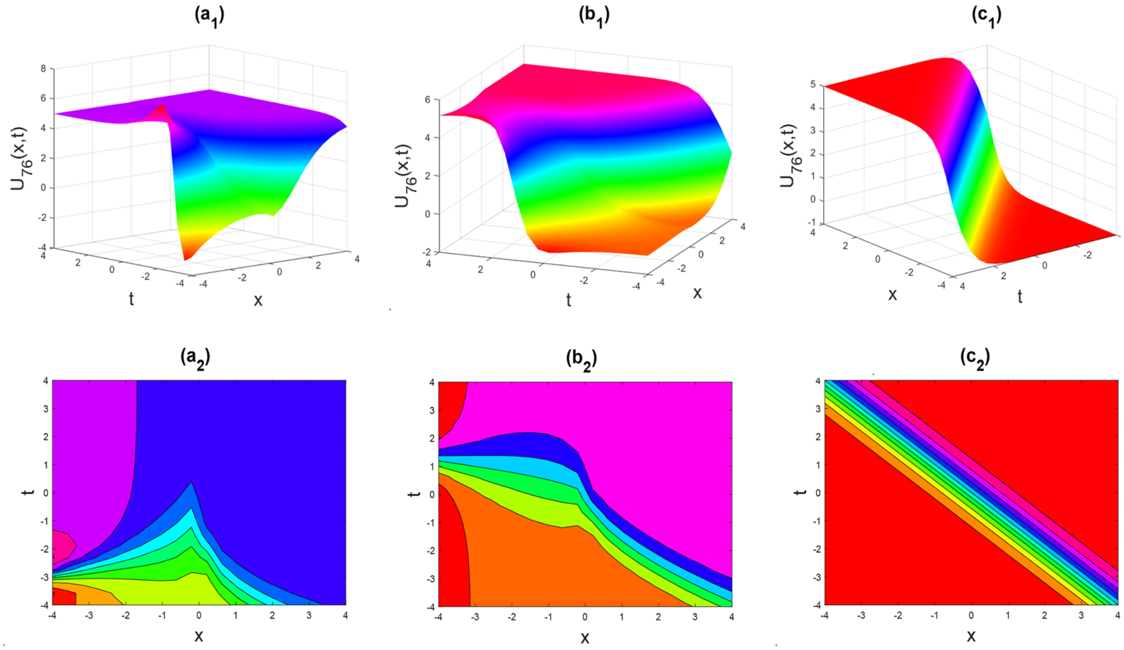

Figure 14. Kink shape of the real part of $U_{76}\left(x, y, t\right)$ for the parameters $a_0 = 1, b_0 = 0.5, \lambda = 1, \mu = 1,$ $y = 0, \theta = 0.3, 0.6, 1.$

Sine-Gordon expansion technique as part of a broader set of tools. Integrate additional perturbation, analytical, or numerical approaches to mitigate the limitations and enhance the method's strengths.

Data availability

The data used to support the findings of this study are available from the corresponding author upon request.

Received: 4 January 2024; Accepted: 19 April 2024
Published online: 24 April 2024

References

1. Alam, L. M. B., Jiang, X. & Al-Mamun, A. Exact and explicit traveling wave solution to the time-fractional phi-four and (2+1) dimensional CBS equations using the modified extended tanh-function method in mathematical physics. *Partial Differ. Equ. Appl. Math.* **4**, 100039 (2021).
2. Rezazadeh, H., Korkmaz, A., Eslami, M., Vahidi, J. & Asghari, R. Traveling wave solution of conformable fractional generalized reaction Duffing model by generalized projective Riccati equation method. *Opt. Quant. Electron.* **50**, 150 (2018).
3. Al-Mamun, A., Ananna, S. N., An, T., Asaduzzaman, M. & Rana, M. S. Sine-Gordon expansion method to construct the solitary wave solutions of a family of 3D fractional WBBM equations. *Results Phys.* **40**, 105845 (2022).
4. Al-Mamun, A., Ananna, S. N., Gharami, P. P., An, T. & Asaduzzaman, M. The improved modified extended tanh-function method to develop the exact travelling wave solutions of a family of 3D fractional WBBM equations. *Results Phys.* **41**, 105969 (2022).
5. Al-Mamun, A. *et al.* An innovative approach for developing the precise traveling wave solutions to a family of 3D fractional WBBM equations. *Partial Differ. Equ. Appl. Math.* **7**, 100522 (2023).
6. Celia, M. A., Bouloutas, E. T. & Zarba, R. L. A general mass-conservative numerical solution for the unsaturated flow equation. *Water Resour. Res.* **26**, 1483–1496 (1990).
7. Richards, L. A. Capillary conduction of liquids through porous mediums. *Physics* **1**, 318–333 (1931).
8. Verbist, G., Weaire, D. & Kraynik, A. M. The foam drainage equation. *J. Phys. Condens. Matter.* **8**, 3715–3731 (1996).
9. Al-Mamun, A. *et al.* Exact and explicit travelling-wave solutions to the family of new 3D fractional WBBM equations in mathematical physics. *Results Phys.* **19**, 103517 (2020).
10. Boakye-Ansah, Y. A. & Grassia, P. Comparing and contrasting travelling wave behaviour for groundwater flow and foam drainage. *Transp. Porous Med.* **137**, 255–280 (2021).
11 Kacimov, A. R. & Šimůnek, J. Analytical traveling-wave solutions and HYDRUS modeling of wet wedges propagating into dry soils: Barenblatt's regime for Boussinesq's equation generalized. *J. Hydrol. (Amst.)* **598**, 126413 (2021).
12 Buenavista, A. J. *et al.* Analytical solutions for the advection-dispersion model for radon-222 production and transport in shallow porewater profiles. *J. Hydrol. (Amst.)* **623**, 129575 (2023).
13. Sokolov, I. M. Physics of fractal operators. *Phys. Today* **56**, 65–66 (2003).
14. Chen, Y., Yan, Z. & Zhang, H. New explicit solitary wave solutions for (2+1)-dimensional Boussinesq equation and (3+1)-dimensional KP equation. *Phys. Lett. A* **307**, 107–113 (2003).
15. Lin, X., Shen, Y., Cai, L. & Ji, R. The distributed system for inverted multi-index visual retrieval. *Neurocomputing* **215**, 241–249 (2016).
16. Mirzazadeh, M. *et al.* Optical solitons and conservation law of Kundu-Eckhaus equation. *Optik (Stuttg)* **154**, 551–557 (2018).
17. Seadawy, A. R. Stability analysis for Zakharov-Kuznetsov equation of weakly nonlinear ion-acoustic waves in a plasma. *Comput. Math. Appl.* **67**, 172–180 (2014).
18 Seadawy, A. R. Stability analysis for two-dimensional ion-acoustic waves in quantum plasmas. *Phys. Plasmas* **21**, 052107 (2014).
19 Alam, L. M. B., Xingfang, J., Al-Mamun, A. & Ananna, S. N. Investigation of lump, soliton, periodic, kink, and rogue waves to the time-fractional phi-four and (2+1) dimensional CBS equations in mathematical physics. *Partial Differ. Equ. Appl. Math.* **4**, 100122 (2021).

20 Al-Mamun, A., Ananna, S. N., An, T. & Foyjonnesa, N. H. M. S. Periodic and solitary wave solutions to a family of new 3D fractional WBBM equations using the two-variable method. *Partial Differ. Equ. Appl. Math.* **3**, 100033 (2021).
21 Al-Mamun, A. *et al.* Dynamical behaviour of travelling wave solutions to the conformable time-fractional modified Liouville and mRLW equations in water wave mechanics. *Heliyon* **7**, e07704 (2021).
22 Al-Mamun, A., Shahen, N. H. M., Ananna, S. N. & Foyjonnesa, M. A. Solitary and periodic wave solutions to the family of new 3D fractional WBBM equations in mathematical physics. *Heliyon* **7**, e07483 (2021).
23. Ananna, S. N., Al-Mamun, A. & An, T. Periodic wave analysis to the time-fractional phi-four and (2+1) dimensional CBS equations. *Int. J. Phys. Res.* **9**, 98–104 (2021).
24 Al-Mamun, A., Ananna, S. N., An, T., Asaduzzaman, M. & Hasan, A. Optical soliton analysis to a family of 3D WBBM equations with conformable derivative via a dynamical approach. *Partial Differ. Equ. Appl. Math.* **5**, 100238 (2022).
25 Foyjonnesa, N. H. M. S., Bashar, M. H., Ali, M. S. & Al-Mamun, A. Dynamical analysis of long-wave phenomena for the nonlinear conformable space-time fractional (2+1)-dimensional AKNS equation in water wave mechanics. *Heliyon* **6**, e05276 (2020).
26 Foyjonnesa, N. H. M. S., Ali, M. S., Al-Mamun, A. & Rahman, M. M. Interaction among lump, periodic, and kink solutions with dynamical analysis to the conformable time-fractional Phi-four equation. *Partial Differ. Equ. Appl. Math.* **4**, 100038 (2021).
27 Al-Mamun, A., Ananna, S. N., An, T., Asaduzzaman, M. & Miah, M. M. Solitary wave structures of a family of 3D fractional WBBM equation via the tanh–coth approach. *Partial Differ. Equ. Appl. Math.* **5**, 100237 (2022).
28. Al-Mamun, A., Asaduzzaman, M. & Ananna, S. N. Solution of eighth order boundary value problem by using variational iteration method. *Int. J. Math. Comput. Sci.* **5**, 13–23 (2019).
29. Al-Mamun, A. & Asaduzzaman, M. Solution of seventh order boundary value problem by using variational iteration method. *Int. J. Math. Comput. Sci.* **5**, 6–12 (2019).
30. Ananna, S. N. & Mamun, A.-A.-. Solution of Volterra's integro-differential equations by using variational iteration method. *Int. J. Sci. Eng. Res.* **11**(3), 1–9 (2020).
31. Mamun, A.-A.-, Ali, M. S. & Miah, M. M. A study on an analytic solution 1D heat equation of a parabolic partial differential equation and implement in computer programming. *Int. J. Sci. Eng. Res.* **9**(9), 913–921 (2018).
32. Hong, X., Manafian, J., Ilhan, O. A., Alkireet, A. I. A. & Nasution, M. K. M. Multiple soliton solutions of the generalized Hirota-Satsuma-Ito equation arising in shallow water wave. *J. Geom. Phys.* **170**, 104338 (2021).
33. Zhang, M., Xie, X., Manafian, J., Ilhan, O. A. & Singh, G. Characteristics of the new multiple rogue wave solutions to the fractional generalized CBS-BK equation. *J. Adv. Res.* **38**, 131–142 (2022).
34. Nisar, K. S. *et al.* Novel multiple soliton solutions for some nonlinear PDEs via multiple Exp-function method. *Results Phys.* **21**, 103769 (2021).
35. Baskonus, H. M. New acoustic wave behaviors to the Davey-Stewartson equation with power-law nonlinearity arising in fluid dynamics. *Nonlinear Dyn.* **86**, 177–183 (2016).
36. Sivasundaram, S., Kumar, A. & Singh, R. K. On the complex properties of the first equation of the Kadomtsev-Petviashvili hierarchy. *Int. J. Math. Comput. Eng.* **2**, 71–84 (2024).
37. Gao, W. & Baskonus, H. M. The modulation instability analysis and analytical solutions of the nonlinear Gross–Pitaevskii model with conformable operator and riemann wave equations via recently developed scheme. *Adv. Math. Phys.* **2023**, 1–16 (2023).
38 Yan, L., Mehmet Baskonus, H., Cattani, C. & Gao, W. Extraction of the gravitational potential and high-frequency wave perturbation properties of nonlinear (3 + 1)-dimensional Vakhnenko-Parkes equation via novel approach. *Math. Methods Appl. Sci.* **47**, 3480–3489 (2024).
39. Ma, W. X. & Fuchssteiner, B. Explicit and exact solutions to a Kolmogorov-Petrovskii-Piskunov equation. *Int. J. Non Linear Mech.* **31**, 329–338 (1996).
40. Mulimani, M. & Kumbinarasaiah, S. A novel approach for Benjamin-Bona-Mahony equation via ultraspherical wavelets collocation method. *Int. J. Math. Comput. Eng.* https://doi.org/10.2478/ijmce-2024-0014 (2024).
41. Hussain, A., Ali, H., Zaman, F. & Abbas, N. New closed form solutions of some nonlinear pseudo-parabolic models via a new extended direct algebraic method. *Int. J. Math. Comput. Eng.* **2**, 35–58 (2024).
42. Kumar, A. & Kumar, S. Dynamic nature of analytical soliton solutions of the (1+1)-dimensional Mikhailov-Novikov-Wang equation using the unified approach. *Int. J. Math. Comput. Eng.* **1**, 217–228 (2023).
43. Mahmud, A. A., Tanriverdi, T. & Muhamad, K. A. Exact traveling wave solutions for (2+1)-dimensional Konopelchenko-Dubrovsky equation by using the hyperbolic trigonometric functions methods. *Int. J. Math. Comput. Eng.* **1**, 11–24 (2023).
44. Ma, W.-X. & Lee, J.-H. A transformed rational function method and exact solutions to the 3+1 dimensional Jimbo-Miwa equation n. *Chaos Solit. Fract.* **42**, 1356–1363 (2009).
45. Zhou, X., Ilhan, O. A., Manafian, J., Singh, G. & Salikhovich Tuguz, N. N-lump and interaction solutions of localized waves to the (2+1)-dimensional generalized KDKK equation. *J. Geom. Phys.* **168**, 104312 (2021).
46 Gu, Y. *et al.* Variety interaction between k-lump and k-kink solutions for the (3+1)-D Burger system by bilinear analysis. *Results Phys.* **43**, 106032 (2022).
47. Ilhan, O. A., Manafian, J. & Shahriari, M. Lump wave solutions and the interaction phenomenon for a variable-coefficient Kadomtsev-Petviashvili equation. *Comput. Math. Appl.* **78**, 2429–2448 (2019).
48. Huang, L., Manafian, J., Singh, G., Nisar, K. S. & Nasution, M. K. M. New lump and interaction soliton, N-soliton solutions and the LSP for the (3 + 1)-D potential-YTSF-like equation. *Results Phys.* **29**, 104713 (2021).
49 Gharami, P. P., Gazi, M. A., Ananna, S. N. & Ahmmed, S. F. Numerical exploration of MHD unsteady flow of THNF passing through a moving cylinder with Soret and Dufour effects. *Partial Differ. Equ. Appl. Math.* **6**, 100463 (2022).
50. Nisar, K. S., Ilhan, O. A., Manafian, J., Shahriari, M. & Soybaş, D. Analytical behavior of the fractional Bogoyavlenskii equations with conformable derivative using two distinct reliable methods. *Results Phys.* **22**, 103975 (2021).
51. Ren, J., Ilhan, O. A., Bulut, H. & Manafian, J. Multiple rogue wave, dark, bright, and solitary wave solutions to the KP–BBM equation. *J. Geom. Phys.* **164**, 104159 (2021).
52. Zhang, H., Manafian, J., Singh, G., Ilhan, O. A. & Zekiy, A. O. N-lump and interaction solutions of localized waves to the (2 + 1)-dimensional generalized KP equation. *Results Phys.* **25**, 104168 (2021).
53. Chen, Z. *et al.* Extracting the exact solitons of time-fractional three coupled nonlinear Maccari's system with complex form via four different methods. *Results Phys.* **36**, 105400 (2022).
54. Kumar, D., Hosseini, K. & Samadani, F. The sine-Gordon expansion method to look for the traveling wave solutions of the Tzitzéica type equations in nonlinear optics. *Optik (Stuttg)* **149**, 439–446 (2017).
55. Korkmaz, A., Hepson, O. E., Hosseini, K., Rezazadeh, H. & Eslami, M. Sine-Gordon expansion method for exact solutions to conformable time fractional equations in RLW-class. *J. King Saud. Univ. Sci.* **32**, 567–574 (2020).
56 Ma, W.-X. & Lee, J.-H. A transformed rational function method and exact solutions to the 3+1 dimensional Jimbo-Miwa equation. *Chaos Solit. Fract.* **42**, 1356–1363 (2009).
57. Ma, W.-X. & Zhou, Y. Lump solutions to nonlinear partial differential equations via Hirota bilinear forms. *J. Differ. Equ.* **264**, 2633–2659 (2018).
58. Yamgoué, S. B., Deffo, G. R. & Pelap, F. B. A new rational sine-Gordon expansion method and its application to nonlinear wave equations arising in mathematical physics. *Eur. Phys. J. Plus* **134**, 1–15 (2019).
59 Leta, T. D., Achab, A. E., Liu, W. & Ding, J. Application of bifurcation method and rational sine-Gordon expansion method for solving 2D complex Ginzburg-Landau equation. *Int. J. Mod. Phys. B* **34**, 2050079 (2020).

60 Kemaloğlu, B., Yel, G. & Bulut, H. An application of the rational sine–Gordon method to the Hirota equation. *Opt. Quant. Electron.* **55**, 658 (2023).

Acknowledgements
This paper was supported by the Water Conservancy Science and Technology Projects of Jiangsu Province, China (No. 2021021).

Author contributions
Data Curation, Software, Writing, Investigation, Formal Analysis [Abdulla - Al - Mamun]; Software, Data Curation, Writing, Formal Analysis [Samsun Nahar Ananna]; Supervision, Writing-Reviewing Editing [Chunhui Lu]; Writing, Formal Analysis [Md Mohi Uddin]. All authors of this paper have read and approved the final version submitted.

Competing interests
The authors declare no competing interests.

Additional information
Correspondence and requests for materials should be addressed to A.-A.M.

Reprints and permissions information is available at www.nature.com/reprints.

Publisher's note Springer Nature remains neutral with regard to jurisdictional claims in published maps and institutional affiliations.